

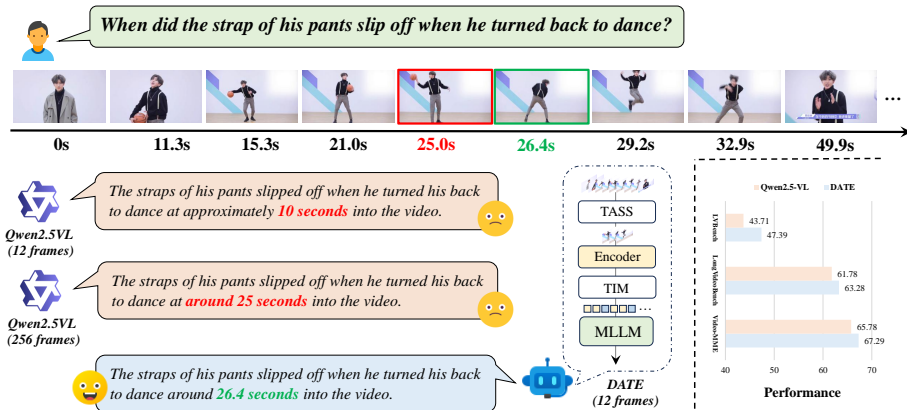
# 000 DATE: DYNAMIC ABSOLUTE TIME ENHANCEMENT 001 FOR LONG VIDEO UNDERSTANDING 002 003 004

005 **Anonymous authors**

006 Paper under double-blind review

## 009 ABSTRACT

011 Long video understanding remains a fundamental challenge for multimodal large  
012 language models (MLLMs), particularly in tasks requiring precise temporal rea-  
013 soning and event localization. Existing approaches typically adopt uniform frame  
014 sampling and rely on implicit position encodings to model temporal order. How-  
015 ever, these methods struggle with long-range dependencies, leading to critical  
016 information loss and degraded temporal comprehension. In this paper, we propose  
017 **Dynamic Absolute Time Enhancement (DATE)** that enhances temporal awareness  
018 in MLLMs through the Timestamp Injection Mechanism (TIM) and a semantically  
019 guided Temporal-Aware Similarity Sampling (TASS) strategy. Specifically, we  
020 interleave video frame embeddings with textual timestamp tokens to construct a  
021 continuous temporal reference system. We further reformulate the video sampling  
022 problem as a vision-language retrieval task and introduce a two-stage algorithm  
023 to ensure both semantic relevance and temporal coverage: enriching each query  
024 into a descriptive caption to better align with the vision feature, and sampling key  
025 event with a similarity-driven temporally regularized greedy strategy. Our method  
026 achieves remarkable improvements w.r.t. absolute time understanding and key  
027 event localization, resulting in state-of-the-art performance among 7B and 72B  
028 models on hour-long video benchmarks. Particularly, our 7B model even exceeds  
029 many 72B models on some benchmarks.



044 Figure 1: A **Real** example of our proposed DATE compared with Qwen2.5-VL. It shows DATE with  
045 12 frames beats 256 frames of Qwen2.5-VL.  
046

## 047 1 INTRODUCTION

050 Multimodal large language models (MLLMs) Alayrac et al. (2022); Cheng et al. (2024b); Wang et al.  
051 (2024a) have shown remarkable performance in a wide range of video understanding tasks, including  
052 video captioning, question answering, and event localization. However, when extended to long videos,  
053 these models face fundamental challenges in temporal reasoning and precise event localization. The  
essential reason for this limitation lies in the mismatch between rigid input length constraints of

054 transformer architectures and the inherently long and continuous nature of real-world video content.  
 055 As a result, existing approaches typically resort to uniform frame sampling as a preprocessing step.  
 056 Unfortunately, this coarse-grained strategy often leads to the loss of critical visual events, temporal  
 057 discontinuity, and the collapse of causality chains, severely limiting the model’s capacity to reason  
 058 over spatiotemporal structures. Moreover, there is no ability to perform perception and alignment of  
 059 the absolute time and the corresponding frames.

060 One major obstacle is the inability of current methods to construct explicit representations of **absolute**  
 061 **time**. Even when time-stamped subtitles are used as prompts, models struggle to align absolute  
 062 timestamps with specific video frames. Although models such as Qwen2.5VLBai et al. (2025)  
 063 incorporate absolute time information into the temporal position embedding based on Multimodal  
 064 RoPEWang et al. (2024a); Su et al. (2024), this approach exhibits critical drawbacks: For short video  
 065 clips, time differences within one second remain indistinguishable; for long videos, the continual  
 066 growth of positional indices leads to a loss of relative positional perception and eventual degradation  
 067 of temporal comprehension. Our diagnostic experiments further confirm that such models do not  
 068 solve problems related to absolute time reliably.

069 Another significant challenge comes from frame sampling itself. Uniform discretizations of frames  
 070 lead to sparse observations, especially in long videos where adjacent frames may be separated by  
 071 tens of seconds. Such sampling is agnostic to semantic content and fails to adapt dynamically to  
 072 user queries, resulting in low recall when critical events are temporally sparse. Recent methods  
 073 like Adaptive Keyframe Selection (AKS)Tang et al. (2025) attempt to mitigate this by introducing  
 074 query-guided dynamic sampling. However, they suffer from two key issues: (1) they use raw user  
 075 questions as CLIPRadford et al. (2021) text encoders, which contradicts CLIP’s training paradigm  
 076 centered on descriptive captions, leading to unstable or truncated representations; (2) their sampling  
 077 method may still select irrelevant frames (e.g., negative samples with relatively high scores) and often  
 078 fails in visually stable segments due to insufficient score variance.

079 To address these limitations, we proposed DATE, as shown in Fig.2, for absolute time-aware video  
 080 understanding and event localization. Our method builds a temporal coordinate system directly within  
 081 the multimodal sequence by interleaving explicit timestamp tokens with video frame embeddings.  
 082 This timestamp injection preserves visual continuity while allowing for precise and controllable  
 083 temporal references. To guide the model towards relevant content, we formulate video sampling as a  
 084 text-image retrieval task and employ a two-stage semantic-guided selection strategy: (i) rewriting  
 085 user questions into caption-style descriptions for better alignment with CLIP-based vision-language  
 086 similarity computation, and (ii) applying a temporally-regularized greedy sampling algorithm that  
 087 ensures both high semantic relevance and temporal diversity. Our contributions are three-folds:  
 088

- (1) We introduce **Timestamp Injection Mechanism (TIM)** that enables explicit absolute time  
 089 modeling without modifying model weights or requiring additional training.
- (2) We propose **Temporally-Aware Similarity Sampling (TASS)**, a temporally-regularized greedy  
 090 sampling algorithm with semantic-guided caption generation to sample frames, which balance key  
 091 events with video continuity.
- (3) We show that our method achieves superior **spatial perception** and **event localization**, especially  
 092 for **hour-long** video scenarios, which achieve SOTA on 7B models, even surpassing many 72B  
 093 models. Moreover, the DATE-72B model achieves state-of-the-art performance.

094

## 095 2 RELATED WORKS

096

### 097 2.1 MULTIMODAL LARGE LANGUAGE MODELS FOR VIDEO UNDERSTANDING

098

099 With the widespread success of large language models (LLMs) Achiam et al. (2023); Brown et al.  
 100 (2020); Chiang et al. (2023); Chowdhery et al. (2023); Chung et al. (2024); Grattafiori et al. (2024);  
 101 Touvron et al. (2023a;b); Ray (2023); Chen et al. (2024c) in natural language processing, researchers  
 102 have extended these models to multimodal scenarios, forming multimodal large language models  
 103 (MLLMs)Lai et al. (2024); Liu et al. (2023). By incorporating visual encoders, MLLMs are capable  
 104 of processing visual inputs such as images or videos, enabling tasks like visual question answering,  
 105 video captioning, and visual reasoningMaaz et al. (2023); Alayrac et al. (2022); Chen et al. (2024a);  
 106 Wu et al. (2024a); Min et al. (2024); Qian et al. (2024); Wang et al. (2022). Representative models  
 107

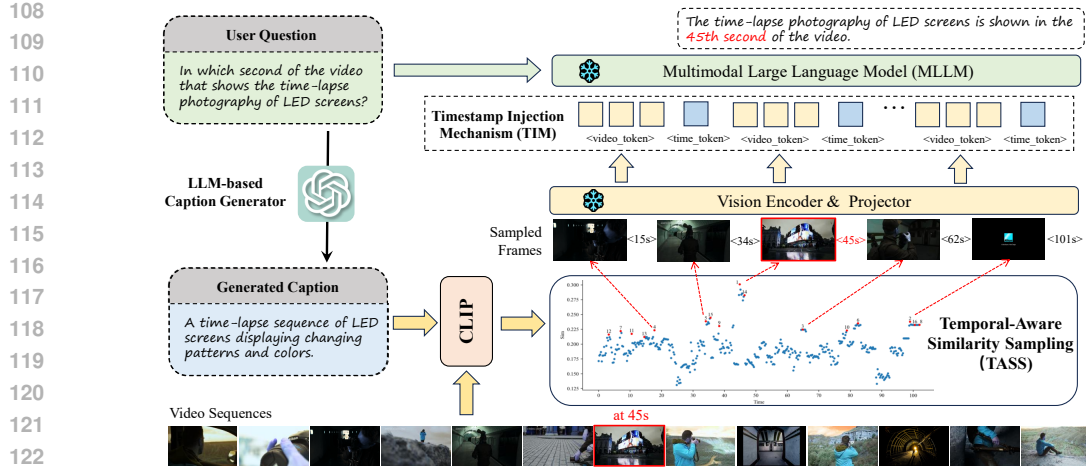


Figure 2: Overview of the proposed framework. For each user input question, using LLM-based Caption Generator to generate a CLIP-aligned image caption, and calculate the similarity with video frames. Then, use Temporal-Aware Similarity Sampling (TASS) strategy to sample the frames (The real sampled frames and orders of this demo could be found in [Appendix B](#)). Last, with Timestamp Injection Mechanism (TIM), we embed timestamps aligned with each frame.

include Video-ChatGPTMaaz et al. (2023); Lin et al. (2023), LLaVA-VideoZhang et al. (2024b), VideoLLAMAZhang et al. (2023); Cheng et al. (2024b); Zhang et al. (2025), and Qwen-VLWang et al. (2024a); Bai et al. (2025), which typically encode video frames into visual tokens and feed them into the model alongside textual tokens. However, due to the inherent context length limitations of LLMs, these models often rely on fixed frame sampling strategies, resulting in significant information compression when processing long video dataFu et al. (2024); Wu et al. (2024b); Wang et al. (2024b). Moreover, long videos present unique challenges such as sparse events and wide semantic spans, which demand more effective temporal modeling and cross-segment reasoning capabilities. Therefore, many strategies Shang et al. (2024); Zhang et al. (2024a); Wei & Chen (2024); Chen et al. (2024d); Wang et al. (2025); Cheng et al. (2024a); He et al. (2024b;a) proposed for longer context.

## 2.2 TEMPORAL MODELING

Temporal modeling is a fundamental challenge in long video understanding. Existing methods can be broadly categorized into two groups: ①Using data with timestamps to fine-tune model with time tokensChen et al. (2024b) or prompts with timestampsRen et al. (2024). These need more data and training cost. ②Explicit incorporation of time into positional encoding. For example, Qwen2.5VL introduces MRoPEBai et al. (2025) and Qwen2.5-OmniXu et al. (2025) introduces TMRoPE, which use absolute time signals into its rotary positional encoding. However, this encoding mechanism is prone to positional drift in long sequences, where the encoded position values grow too quickly with sequence length, thereby distorting the relative temporal relationships between frames. This can reduce the ability of the model to capture temporal causality and duration. More importantly, these methods often fail to provide a stable temporal awareness, thus limiting the ability of the model to perceive absolute time.

## 2.3 FRAME SAMPLING STRATEGY

To mitigate the performance bottleneck caused by limited input length, frame sampling has become a crucial component in video understanding systems. The most common strategy is uniform samplingBai et al. (2025); Cheng et al. (2024b); Li et al. (2024), which is straightforward but fails to adaptively select frames based on semantic importance. This often leads to omission of critical content, especially in videos with dense or uneven event distributions. To address this, some semantics-aware frame selection methods with VLMs like CLIPRadford et al. (2021) have been proposed, such as BOLTIu et al. (2025) and AKSTang et al. (2025), and they proved to be effective over uniform and topk sampling. However, they all use question to find frames, this is not a good

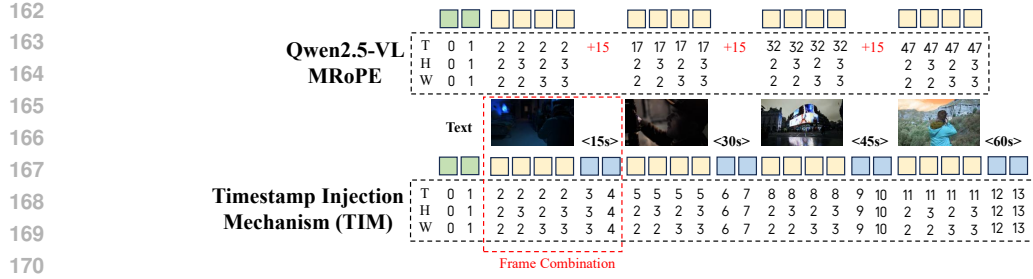


Figure 3: The Multimodal RoPE (MRoPE) with our Timestamp Injection Mechanism (TIM) compared with Qwen2.5-VL’s MRoPE. **Qwen2.5-VL**: Add 15 since there are 15 seconds between frames. **TIM(ours)**: The temporal dimension  $T$  is extended with time token. The spatial dimensions ( $H, W$ ) remain aligned with the first frame, ensuring spatial consistency across the whole sequence.

way for CLIP to embed question, since it was not trained with question. Meanwhile, they may also sample negative frames and loss critical temporal continuity (action, movement, etc.).

### 3 METHODS

#### 3.1 TIMESTAMP INJECTION MECHANISM (TIM)

To enhance the temporal perception of Multimodal Large Language Models (MLLMs) in video understanding, especially in long videos requiring absolute time localization, we propose a timestamp injection mechanism. This mechanism is model-agnostic and compatible with most mainstream MLLMs. In this work, we take Qwen2.5-VLBai et al. (2025), which incorporates explicit absolute time encoding, as our baseline method.

**Token-Level Timestamp Injection** The latest open-source MLLM, Qwen2.5-VL, relies on their proposed MRoPE (Multimodal RoPE) mechanism to model temporal sequences with time interval in the position ID of MRoPEWang et al. (2024a), to embed absolute time of video frames. However, our experiments demonstrate that this approach lacks a true understanding of absolute time.

To address this, we introduce a token-level timestamp injection mechanism. As shown in Fig.3, for each sampled frame, we construct the input sequence using an interleaved structure of visual and time tokens:

```
<video_token><time_token><video_token><time_token> ...<video_token><time_token>
```

Here, each color represents the combination of video tokens and timestamps of a frame, `<video_token>` represents the visual tokens (not one token), and `<time_token>` is its corresponding textual timestamp (e.g., 01 : 23 or 83s). This structure preserves visual continuity while injecting a precise and controllable temporal reference, enabling the language model to perform time-aware reasoning task such as event ordering and absolute time localization.

**Reconstruction of Positional Encoding and Sequential Normalization** The MRoPE mechanism in Qwen2.5-VL introduces absolute time information via position indices in the visual branch. Although it models temporal order to some extent, it suffers from critical limitations when applied to long videos due to linearly increasing position indices(IDs):

**(1) Sparsity and Resource Inefficiency:** Since position IDs grow proportionally, large time gaps (e.g., 20s between frames) leading to inefficient use of the sequence length and potential index explosion (e.g., 10,000 in hour-long videos).

**(2) Degradation of Relative Positional Awareness:** Large gaps between position IDs disrupt the relative distances between tokens, compromising the ability to capture local temporal structures.

To mitigate these issues, we remove the absolute time alignment from Qwen2.5VL’s MRoPE and retain only the original Multimodal RoPE (MRoPE) encoding. Specifically, the temporal dimension  $T$

216 is encoded using a simple *sequential indexing* strategy, where position indices increment according to  
 217 the order of tokens. Furthermore, to preserve the spatial encodings between video frames, we ensure  
 218 that only the temporal dimension  $T$  is extended along with time token insertion. The spatial encodings  
 219 ( $H, W$ ) remain aligned with the first frame, ensuring spatial consistency across the sequence.

220 This design maintains the numerical stability of RoPESu et al. (2024), and preserves the model’s  
 221 sensitivity to token order. Meanwhile, absolute time perception is handled independently via the  
 222 explicit <time\_token>s, resulting in a decoupled and robust time representation framework.  
 223 Moreover, as shown in Fig.6, a modality gap between vision tokens and time tokens makes the model  
 224 can better locate them key events. As the result of the proof in AppendixB.2, when position encoding  
 225 for each frame is less than 6.28, it could perceive relative positions better. Therefore, for ours TIM,  
 226 the video tokens use one position id, and the time token use less than four position ids, which uses a  
 227 total less than five position ids for each frame.

### 229 3.2 TEMPORAL-AWARE SIMILARITY SAMPLING (TASS)

230 Discretized video frame sampling is a common preprocessing step in multimodal video modeling.  
 231 However, in long video scenarios, uniformly spaced sampling strategies exhibit clear limitations.  
 232 On the one hand, the temporal gaps between frames may span several seconds to minutes, making  
 233 it likely to miss sparse but semantically critical moments. On the other hand, uniform sampling is  
 234 task-agnostic, severely undermining the recall of key events.

235 Sampling directly based on similarity leads to frames with little variation being sampled continuously,  
 236 which results in video features collapsing into a single image. Sampling across too large a span would  
 237 then lead to problems with key event continuity, difficulty in recognizing object movement, etc., i.e.,  
 238 a similar problem to that which would occur with uniform sampling and AKSTang et al. (2025).

239 Thus, we proposed **TASS**, a temporally-regularized greedy sampling algorithm that ensures both high  
 240 key event continues and temporal diversity. It consists of two main stages: (i) *semantic-enhanced*  
 241 *similarity computation*, and (ii) *similarity-prioritized sampling under temporal constraints*.

242 **Semantic Enhancement: From Question to Caption** To improve the consistency of the visual-  
 243 language alignment, we first convert the user’s query (typically a question) into a more descriptive  
 244 caption using a language model, and the prompt of this step can be seen in Appendix H. Unlike raw  
 245 questions, captions exhibit a declarative style that aligns better with CLIP’s image-text matching  
 246 paradigm, activating more stable and complete semantic representations.

247 Each video frame  $v_i$  is embedded using CLIP, and its similarity to the caption  $c$  is calculated as:

$$248 s_i = \text{CLIP}(v_i, c) = \frac{\langle v_i, c \rangle}{\|v_i\| \cdot \|c\|} \quad (1)$$

249 **Temporal-Aware Similarity Sampling** We first compute a dynamic threshold  $s_{\text{mean}}$  which is the  
 250 mean of all similarity scores. Scores below the mean are considered *negative samples*, as they  
 251 contribute little to answering the user’s query and are therefore discarded. To ensure computational  
 252 efficiency, we further cap the number of top-ranked candidates by setting an upper bound proportional  
 253 to the final number of selected frames, i.e.,  $\text{topk} \leq 4 \times \text{max\_frames}$ .

$$254 \text{topk} = \min(|\{i \mid s_i > s_{\text{mean}}\}|, \alpha \times \text{max\_frames}) \quad (2)$$

255 where  $\alpha$  is a controllable coefficient. It denotes the number of frames to be sampled (candidate  
 256 frames). For example, Qwen2.5-VL-7B can process up to 256 frames, and we set  $\alpha = 4$  by default,  
 257 using our sampling strategy, we can effectively compress and select representative frames from a  
 258 sequence of  $4 * 256 = 1024$  frames. When negative sample filtering is considered, the expected  
 259 number of candidate frames for sampling could be 2048.

260 While many continuous frames are semantically aligned, they often cluster temporally, leading to  
 261 redundancy. To ensure temporal diversity while preserving semantic relevance, we introduce a greedy  
 262 selection algorithm that is similarity first with enforcing a minimum time interval  $\delta$  between selected  
 263 timestamps. If fewer than  $N_{\text{max}}$  frames are obtained,  $\delta$  is iteratively decayed until the quota is met.  
 264 The pseudo-code is as follows:

---

270 **Algorithm 1** Temporal-Aware Similarity Sampling (TASS)  
271 **Require:** Top-K timestamps  $\mathcal{I}_{\text{topK}}$ , sampled frames  $N_{\text{max}}$ , initial interval  $\delta_0$   
272 **Ensure:** Selected timestamps  $\mathcal{S}_t$

273 1: Initialize  $\mathcal{S}_t \leftarrow \emptyset$ ,  $\delta \leftarrow \delta_0$ , decay ratio  $\lambda = 0.5$   
274 2: **while**  $|\mathcal{S}_t| < N_{\text{max}}$  **do**  
275 3:     **for** each  $t_k \in \mathcal{I}_{\text{topK}}$  **do**  
276 4:         **if**  $\forall t_j \in \mathcal{S}_t, |t_k - t_j| \geq \delta$  or  $\mathcal{S}_t = \emptyset$  **then**  
277 5:              $\mathcal{S}_t \leftarrow \mathcal{S}_t \cup \{t_k\}$   
278 6:             Remove  $t_k$  from  $\mathcal{I}_{\text{topK}}$   
279 7:         **if**  $|\mathcal{S}_t| \geq N_{\text{max}}$  **then**  
280 8:             **break**  
281 9:         **end if**  
282 10:         **end if**  
283 11:     **end for**  
284 12:      $\delta \leftarrow \delta \cdot \lambda$   
285 13: **end while**  
286 14: **return** sorted  $\mathcal{S}_t$

---

286 The most relevant work w.r.t. TASS is the Adaptive Keyframe Selection (AKS) proposed by Tang  
287 et al. Tang et al. (2025), which introduces a query-driven sampling mechanism. However, it suffers  
288 from two major issues: (1) It directly uses raw questions as CLIP text inputs, misaligned with CLIP’s  
289 caption-style since it was trained with image-caption pairs but not questions, and prone to semantic  
290 truncation due to the input limitation; (2) Its variance-based sampling strategy tends to include false  
291 positives (i.e., high-scoring frames from negative segments), due to the small magnitude of score  
292 variations, and may miss keyframes in visually smooth regions.

293 In contrast, our method leverages caption rewriting for better alignment and introduces a temporal  
294 regularization mechanism to ensure broader temporal coverage. This makes sampling more robust  
295 and effective for modeling temporally distributed events in long videos.

## 296 4 EXPERIMENTS

### 299 4.1 BENCHMARKS

300 To comprehensively evaluate our proposed DATE on long video understanding, we conduct ex-  
301 periments on three hour-long video benchmarks that emphasize complex temporal reasoning and  
302 long-context modeling:

304 **Video-MME** Fu et al. (2024) is a video evaluation benchmark designed for general video understand-  
305 ing. It contains 900 videos (256 hours in total) across various categories and durations, annotated with  
306 2,700 expert-curated multiple-choice QA pairs. The dataset is partitioned into short (<2 min), medium  
307 (4–15 min), and long (30–60 min) subsets, enabling a detailed analysis of temporal scalability.

308 **LongVideoBench** Wu et al. (2024b) focuses on long-context multimodal reasoning. It comprises  
309 3,763 videos of up to 1 hour in length and 6,678 annotated questions across 17 categories. The  
310 benchmark emphasizes fine-grained temporal retrieval and localized event reasoning, making it ideal  
311 for evaluating absolute time comprehension.

312 **LBench** Wang et al. (2024b) is one of the most challenging benchmarks for long video understanding,  
313 with an average video length of over 4,000 seconds. It provides 1,549 QA pairs including multiple  
314 tasks such as entity tracking, temporal grounding, and causal reasoning, offering a comprehensive  
315 testbed for temporal-aware video modeling.

316 **Implementation Details** We adopt Qwen2.5-VL (7B and 72B) Bai et al. (2025) as our baseline model.  
317 For fair comparison and reproducibility, we utilize the publicly released checkpoints and re-evaluated  
318 all benchmarks following their official technical report. Our DATE also follows the same settings. In  
319 the evaluation, the baseline adopts a uniform sampling rate of 4 FPS, with the resolution set to 448  
320 (longest side) and a maximum of 256 input frames across all benchmarks. All the experiments are  
321 conducted with Nvidia A100-80G GPUs. For our proposed TASS, deepseek-v3 Liu et al. (2024) is  
322 used for caption generation. Then, the frames are extracted with 1 FPS for all videos to calculate the  
323 visual-textual similarity score with the generated caption. Visual-textual similarity is computed using  
the CLIP ViT-B/32 Radford et al. (2021) model to enable the semantic-aware frame filtering. In the

324  
 325 Table 1: Performance comparison on long video benchmark with SOTAs, including Video-MME  
 326 (w/o subtitles), LongVideoBench, and LVbench. For fairly comparison, we re-test the model based  
 327 on the technical report disclosed by QwenVL team, with all video inputs preprocessed based on  
 328 4FPS and 448 resolution. (♣: official reported results. ♡: we re-test results). In the test, we found  
 329 that the metric reported by QwenVL team on LongVideoBench were tested at 224 resolution. More  
 330 experiments on different model could be found in AppendixC.

331 Models	332 Size	333 Frames	334 Video-MME (w/o sub)		335 LongVideoB	336 LVbench
			337 Long	338 Overall	339 val	340 val
341 <i>Closed Video MLLMs</i>						
342 GLM-4V-Plus	-	256	-	70.8	-	58.7
343 GPT-4o	-	384	65.3	71.9	66.7	27
344 Gemini-1.5-Pro	-	1/0.5fps	67.4	75	64	33.1
345 <i>Open-source Video MLLMs&gt;70B</i>						
346 LLaVA-OneVision-72B	72B	32	-	66.2	61.3	-
347 LLaVA-Video	72B	64	61.5	70.6	61.9	-
348 Qwen2-VL	72B	768	62.2	71.2	60.4	41.3
349 InternVL2.5-78B	78B	16-64	-	72.1	63.6	-
350 InternVL3-78B	78B	16-64	-	72.7	65.7	-
351 Qwen2.5-VL-72B♣	72B	768	-	73.3	60.7	47.3
352 Qwen2.5-VL-72B♦	72B	256	63.4	72.7	66.9	48.8
353 <b>DATE-72B(Ours)</b>	72B	256	<b>65.3</b>	<b>73.3</b>	<b>68.1</b>	<b>52.1</b>
354 <i>Small Video MLLMs</i>						
355 VITA-1.5	7B	16	47.1	56.1	-	-
356 LLaVA-Video	7B	64	-	63.3	58.2	-
357 NVILA	8B	256	54.8	64.2	57.7	-
358 ByteVideoLLM	14B	256	56.4	64.6	-	-
359 VideoLLaMA3	7B	180	-	66.2	59.8	45.3
360 InternVL3-8B	8B	16-64	-	66.3	58.8	-
361 Qwen2.5-VL-7B♣	7B	256	-	65.1	56.0 <sub>224dpi</sub>	45.3
362 Qwen2.5-VL-7B♦	7B	256	55.4	65.8	61.8 <sub>448dpi</sub>	43.7
363 <b>DATE-7B(Ours)</b>	7B	256	<b>57.3</b>	<b>67.3</b>	<b>63.3</b>	<b>47.4</b>

352 **Source:** LVBench (Hf-n1yfd8II.mp4)



353 **Question:**

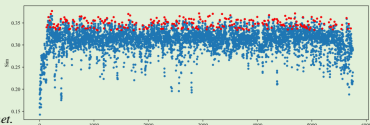
354 *How to describe the feeling of Lee Chong Wei at 48:16?*

355 **Options:**

- 356 A. He feels frustrated because he does not catch the shuttlecock from the opponent
- 357 B. He feels excited because he gets one point
- 358 C. He feels frustrated because he beats the shuttlecock out of bounds
- 359 D. He feels frustrated because he does not beat the shuttlecock cross the net.

360 **Generated Caption:**

361 *Lee Chong Wei's expression, body posture, and reaction after hitting the shuttlecock.*



362 *Qwen2.5-VL: C* *Sampled Frames*

363 *DATE (ours): A*

364 Figure 4: A real demo compared DATE-7B with Qwen2.5-VL-7B. The caption is generated with our  
 365 method and calculate similarity scores with frames. The red points are sampled frames with TASS.  
 366 More could be found in **Appendix**.

367 TASS (Temporal-Aware Similarity Sampling) module, we set the selection ratio coefficient  $\alpha = 4$ ,  
 368 and initialize the temporal interval constraint  $\delta_0$  to 20 seconds.

## 371 4.2 MAIN RESULTS

373 **Comparison with the State-of-the-Art** We compare our proposed method, DATE, with a variety  
 374 of state-of-the-art closed-source and open-source video MLLMs on multiple long-video benchmarks,  
 375 as summarized in Table 4. Compared to other small-scale video MLLMs, DATE achieves consistent  
 376 improvements across all benchmarks, outperforming the prior best model (Qwen2.5-VL) by +1.5%  
 377 on Video-MME (Overall), +1.5% on LongVideoBench (val), and +2.1% on LVbench (An extremely  
 long video benchmark). Moreover, our method (256 frames) even outperforms the Qwen2.5-VL-72B

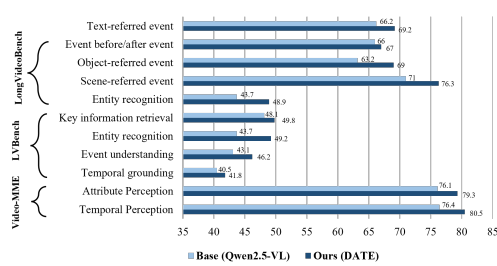


Figure 5: Comparison of performance related to event-aware tasks in the three benchmarks: Video-MME, LongVideoBench, and LVbench.

Table 2: Ablation study on two components of DATE-7B on three long video benchmarks: Video-MME, LongVideoBench, and LVbench.

TIM	TASS	V-MME	LongVideoB	LVb
✗	✗	65.8	61.8	43.7
✓	✗	66.5	61.9	44.9
✗	✓	66.6	62.8	46.7
✓	✓	<b>67.3</b>	<b>63.3</b>	<b>47.4</b>

Table 3: Comparisons with latest methods on LVbench. The baseline is the Qwen2.5-VL-7B model with uniform sampling and their MRoPE. **Sampling Strategy:** we compared TASS with AKS (most latest method), and list the computation time for both methods under the same CPU. **Time Embedding:** We compared our method TIM with timestamps given in prompt.

Frames	Base	SamplingStrategy		Time Embedding	
		TASS(Ours)	AKSTang et al. (2025)	TIM(Ours)	Prompt
256	43.7	<b>46.7</b>	21.2s	45.8	21.1s
128	40.7	<b>45.8</b>	6.4s	44.6	19.2s
64	38.8	42.6	2.7s	<b>43.3</b>	16.4s
32	36.8	<b>40.9</b>	1.7s	39.6	13.9s
16	33.9	<b>39.8</b>	1.2s	33.8	11.7s

(768 frames) model on LongVideoBench and LVbench. These gains demonstrate DATE’s superior temporal modeling capability, especially in handling extremely long videos. It shows our methods effectively injects temporal cues and helps the model focus on semantically important moments, enabling more robust long-range reasoning.

**Comparison with Event-aware tasks.** To better understand the advantage of DATE in modeling temporal and event-centric information, we provide a detailed comparison across fine-grained sub-tasks in Video-MME, LVbench, and LongVideoBench, as shown in Figure 5.

#### 4.3 PRECISE EVENT LOCALIZATION CAPABILITIES

Our DATE shows significant advantages in accurate event localization. As shown in the Fig.1, DATE can accurately identify the specific time points of events even when only 12 frames are used, and even accurately samples the critical time with only one frame as shown by the sampling order labeled in the sampling graph. However, the baseline model still shows significant deviations at 256 frames. This validates the effectiveness and robustness of our proposed temporal modeling and semantic-driven sampling strategy for long video understanding. Fig.4 also shows some cases in benchmarks, more examples can be found in the **Appendix**.

#### 4.4 ABLATION STUDIES

We conduct comprehensive ablation studies to evaluate the two core components in DATE: Timestamp Injection Mechanism (TIM) and Temporal-Aware Similarity Sampling (TASS) on Video-MME, LongVideoBench, and LVbench, which are reported in Table 2.

To further analyze the effectiveness and efficiency of our sampling method, we compare TASS with Adaptive Keyframe Selection (AKS) Tang et al. (2025), a recent method proposed at CVPR’25, under large range of frame rates (**from 16 to 256**). As shown in Table3, TASS consistently outperforms AKS across nearly all frame settings, especially at lower frame counts (e.g., +6.0% at 16 frames),

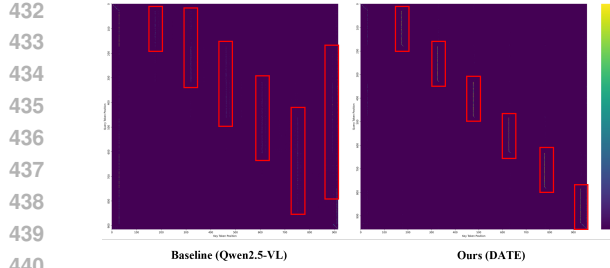


Figure 6: Attention maps of Qwen2.5-VL and our TIM with 6 times token. Rectangles label the attention area of each frame’s vision tokens. TIM binds times to the corresponding frame and lead to a scope constraint on attentions.

while achieving comparable or even faster sampling times on the same CPU. These results highlight the efficiency and effectiveness of our sampling design.

Moreover, TIM consistently outperforms the simple "timestamp-in-prompt" method, demonstrating that directly embedding temporal cues into the token space is a more effective way to inject temporal awareness into MLLMs than relying on implicit prompt descriptions.

#### 4.5 TIM ATTENTION ANALYSIS

To investigate the impact of temporal information on video understanding, we visualize attention maps of the baseline and our TIM. This experiment is conducted on the demo from Fig.1, using 12 input frames. Since Qwen2.5-vl merges every 2 frames, a total of 6 timestamp tokens are embedded.

As shown in Fig.6 (left), the baseline exhibits a relatively diffuse attention pattern, indicating that the model relies mainly on content-based similarity across the sequence. In contrast, the attention map of DATE (Fig.6, right) reveals a distinct pattern. Notably, video tokens corresponding to the timestamp receive significantly higher attention, suggesting that timestamp tokens act as temporal anchors. They enable the model to associate specific moments with the broader video content.

Furthermore, the explicit temporal cues introduced by timestamp tokens appear to improve the ability to localize frame information. By offering a temporal reference frame for aggregating content across the sequence, the model enhances its contextual understanding of individual video segments.

#### 4.6 HYPER-PARAMETERS ANALYSIS

As shown in Fig.7  $\alpha$  controls the number of candidate frames, acting as an effective filtering mechanism to remove distracting information, it achieves the best performance at 4;  $\delta_0$  constrains the initial temporal range of sampling, demonstrating the stability of the algorithm, which samples well no matter how it is initialized, ensuring continuity between frames and enhancing coverage of key events. Experimental results demonstrate that with appropriate configurations, TASS achieves a good balance between efficiency and temporal awareness.

## 5 CONCLUSION

In this work, we propose DATE, designed to enhance absolute time understanding and event localization in long videos for Multimodal Large Language Models (MLLMs). By timestamp tokens injection mechanism (TIM) and a semantic-driven key event sampling strategy (TASS), our method constructs an explicit and continuous temporal coordinate model with a Plug-and-Play way. Extensive experiments on multiple long-video benchmarks demonstrate that DATE significantly improves the model’s ability to identify and align over temporally grounded events. Our findings highlight the importance of precise time modeling and open new direction to enhance time awareness for MLLMs.

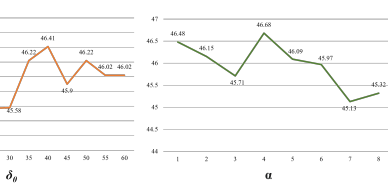


Figure 7: Hyper-parameters analysis of TASS.  $\delta_0$  is the initial minimum time interval for sampling, and  $\alpha$  controls the candidate sampling frames.

486 6 REPRODUCIBILITY STATEMENT  
487488 Our method is a plug-and-play method, so that everyone can reproduce the same results as shown in  
489 the paper.  
490491 7 ETHICS STATEMENT  
492493 We do not encounter any ethical concerns, as our work is conducted entirely on publicly available  
494 models and benchmarks:  
495496 

- **Benchmark:** Video-MME (Allows to used for academic research)
- **Benchmark:** LongVideoBench (CC-BY-NC-SA 4.0 license)
- **Benchmark:** LongVideoBench (CC-BY-NC-SA 4.0 license)
- **Model:** Qwen2.5-VL (Apache-2.0 license)
- **Compliance:** No private or proprietary assets were used. All usages comply with academic  
research standards and ethical guidelines.

  
503504 REFERENCES  
505506 Josh Achiam, Steven Adler, Sandhini Agarwal, Lama Ahmad, Ilge Akkaya, Florencia Leoni Aleman,  
507 Diogo Almeida, Janko Altenschmidt, Sam Altman, Shyamal Anadkat, et al. Gpt-4 technical report.  
508 *arXiv preprint arXiv:2303.08774*, 2023.509 Jean-Baptiste Alayrac, Jeff Donahue, Pauline Luc, Antoine Miech, Iain Barr, Yana Hasson, Karel  
510 Lenc, Arthur Mensch, Katherine Millican, Malcolm Reynolds, et al. Flamingo: a visual language  
511 model for few-shot learning. *Advances in neural information processing systems*, 35:23716–23736,  
512 2022.513 Shuai Bai, Keqin Chen, Xuejing Liu, Jialin Wang, Wenbin Ge, Sibo Song, Kai Dang, Peng Wang,  
514 Shijie Wang, Jun Tang, et al. Qwen2. 5-vl technical report. *arXiv preprint arXiv:2502.13923*,  
515 2025.516 Tom Brown, Benjamin Mann, Nick Ryder, Melanie Subbiah, Jared D Kaplan, Prafulla Dhariwal,  
517 Arvind Neelakantan, Pranav Shyam, Girish Sastry, Amanda Askell, et al. Language models are  
518 few-shot learners. *Advances in neural information processing systems*, 33:1877–1901, 2020.519 Lin Chen, Xilin Wei, Jinsong Li, Xiaoyi Dong, Pan Zhang, Yuhang Zang, Zehui Chen, Haodong Duan,  
520 Zhenyu Tang, Li Yuan, et al. Sharegpt4video: Improving video understanding and generation with  
521 better captions. *Advances in Neural Information Processing Systems*, 37:19472–19495, 2024a.522 Shimin Chen, Xiaohan Lan, Yitian Yuan, Zequn Jie, and Lin Ma. Timemarker: A versatile video-llm  
523 for long and short video understanding with superior temporal localization ability. *arXiv preprint*  
524 *arXiv:2411.18211*, 2024b.525 Shimin Chen, Yitian Yuan, Shaoxiang Chen, Zequn Jie, and Lin Ma. Fewer tokens and fewer  
526 videos: Extending video understanding abilities in large vision-language models. *arXiv preprint*  
527 *arXiv:2406.08024*, 2024c.528 Yukang Chen, Fuzhao Xue, Dacheng Li, Qinghao Hu, Ligeng Zhu, Xiuyu Li, Yunhao Fang, Haotian  
529 Tang, Shang Yang, Zhijian Liu, et al. Longvila: Scaling long-context visual language models for  
530 long videos. *arXiv preprint arXiv:2408.10188*, 2024d.531 Dingxin Cheng, Mingda Li, Jingyu Liu, Yongxin Guo, Bin Jiang, Qingbin Liu, Xi Chen, and  
532 Bo Zhao. Enhancing long video understanding via hierarchical event-based memory. *arXiv*  
533 *preprint arXiv:2409.06299*, 2024a.534 Zesen Cheng, Sicong Leng, Hang Zhang, Yifei Xin, Xin Li, Guanzheng Chen, Yongxin Zhu, Wenqi  
535 Zhang, Ziyang Luo, Deli Zhao, et al. Videollama 2: Advancing spatial-temporal modeling and  
536 audio understanding in video-llms. *arXiv preprint arXiv:2406.07476*, 2024b.

540 Wei-Lin Chiang, Zhuohan Li, Ziqing Lin, Ying Sheng, Zhanghao Wu, Hao Zhang, Lianmin Zheng,  
 541 Siyuan Zhuang, Yonghao Zhuang, Joseph E Gonzalez, et al. Vicuna: An open-source chatbot  
 542 impressing gpt-4 with 90%\* chatgpt quality. See <https://vicuna.lmsys.org> (accessed 14 April  
 543 2023), 2(3):6, 2023.

544 Aakanksha Chowdhery, Sharan Narang, Jacob Devlin, Maarten Bosma, Gaurav Mishra, Adam  
 545 Roberts, Paul Barham, Hyung Won Chung, Charles Sutton, Sebastian Gehrmann, et al. Palm:  
 546 Scaling language modeling with pathways. *Journal of Machine Learning Research*, 24(240):1–113,  
 547 2023.

548 Hyung Won Chung, Le Hou, Shayne Longpre, Barret Zoph, Yi Tay, William Fedus, Yunxuan Li,  
 549 Xuezhi Wang, Mostafa Dehghani, Siddhartha Brahma, et al. Scaling instruction-finetuned language  
 550 models. *Journal of Machine Learning Research*, 25(70):1–53, 2024.

552 Chaoyou Fu, Yuhua Dai, Yongdong Luo, Lei Li, Shuhuai Ren, Renrui Zhang, Zihan Wang, Chenyu  
 553 Zhou, Yunhang Shen, Mengdan Zhang, et al. Video-mme: The first-ever comprehensive evaluation  
 554 benchmark of multi-modal llms in video analysis. *arXiv preprint arXiv:2405.21075*, 2024.

555 Aaron Grattafiori, Abhimanyu Dubey, Abhinav Jauhri, Abhinav Pandey, Abhishek Kadian, Ahmad  
 556 Al-Dahle, Aiesha Letman, Akhil Mathur, Alan Schelten, Alex Vaughan, et al. The llama 3 herd of  
 557 models. *arXiv preprint arXiv:2407.21783*, 2024.

559 Bo He, Hengduo Li, Young Kyun Jang, Menglin Jia, Xuefei Cao, Ashish Shah, Abhinav Shrivastava,  
 560 and Ser-Nam Lim. Ma-lmm: Memory-augmented large multimodal model for long-term video  
 561 understanding. In *Proceedings of the IEEE/CVF Conference on Computer Vision and Pattern  
 562 Recognition*, pp. 13504–13514, 2024a.

563 Yefei He, Feng Chen, Jing Liu, Wenqi Shao, Hong Zhou, Kaipeng Zhang, and Bohan Zhuang.  
 564 Zipvl: Efficient large vision-language models with dynamic token sparsification and kv cache  
 565 compression. *arXiv preprint arXiv:2410.08584*, 2024b.

566 Xin Lai, Zhuotao Tian, Yukang Chen, Yanwei Li, Yuhui Yuan, Shu Liu, and Jiaya Jia. Lisa: Reasoning  
 567 segmentation via large language model. In *Proceedings of the IEEE/CVF Conference on Computer  
 568 Vision and Pattern Recognition*, pp. 9579–9589, 2024.

570 Bo Li, Yuanhan Zhang, Dong Guo, Renrui Zhang, Feng Li, Hao Zhang, Kaichen Zhang, Peiyuan  
 571 Zhang, Yanwei Li, Ziwei Liu, et al. Llava-onevision: Easy visual task transfer. *arXiv preprint  
 572 arXiv:2408.03326*, 2024.

573 Bin Lin, Yang Ye, Bin Zhu, Jiaxi Cui, Munan Ning, Peng Jin, and Li Yuan. Video-llava: Learning  
 574 united visual representation by alignment before projection. *arXiv preprint arXiv:2311.10122*,  
 575 2023.

577 Aixin Liu, Bei Feng, Bing Xue, Bingxuan Wang, Bochao Wu, Chengda Lu, Chenggang Zhao,  
 578 Chengqi Deng, Chenyu Zhang, Chong Ruan, et al. Deepseek-v3 technical report. *arXiv preprint  
 579 arXiv:2412.19437*, 2024.

580 Haotian Liu, Chunyuan Li, Qingyang Wu, and Yong Jae Lee. Visual instruction tuning. *Advances in  
 581 neural information processing systems*, 36:34892–34916, 2023.

582 Shuming Liu, Chen Zhao, Tianqi Xu, and Bernard Ghanem. Bolt: Boost large vision-language model  
 583 without training for long-form video understanding. *arXiv preprint arXiv:2503.21483*, 2025.

585 Muhammad Maaz, Hanooona Rasheed, Salman Khan, and Fahad Shahbaz Khan. Video-chatgpt:  
 586 Towards detailed video understanding via large vision and language models. *arXiv preprint  
 587 arXiv:2306.05424*, 2023.

588 Juhong Min, Shyamal Buch, Arsha Nagrani, Minsu Cho, and Cordelia Schmid. Morevqa: Exploring  
 589 modular reasoning models for video question answering. In *Proceedings of the IEEE/CVF  
 590 Conference on Computer Vision and Pattern Recognition*, pp. 13235–13245, 2024.

591 Long Qian, Juncheng Li, Yu Wu, Yaobo Ye, Hao Fei, Tat-Seng Chua, Yuetong Zhuang, and Siliang  
 592 Tang. Momentor: Advancing video large language model with fine-grained temporal reasoning.  
 593 *arXiv preprint arXiv:2402.11435*, 2024.

594 Alec Radford, Jong Wook Kim, Chris Hallacy, Aditya Ramesh, Gabriel Goh, Sandhini Agarwal,  
 595 Girish Sastry, Amanda Askell, Pamela Mishkin, Jack Clark, et al. Learning transferable visual  
 596 models from natural language supervision. In *International conference on machine learning*, pp.  
 597 8748–8763. PMLR, 2021.

598 Partha Pratim Ray. Chatgpt: A comprehensive review on background, applications, key challenges,  
 599 bias, ethics, limitations and future scope. *Internet of Things and Cyber-Physical Systems*, 3:  
 600 121–154, 2023.

602 Shuhuai Ren, Linli Yao, Shicheng Li, Xu Sun, and Lu Hou. Timechat: A time-sensitive multimodal  
 603 large language model for long video understanding. In *Proceedings of the IEEE/CVF Conference*  
 604 *on Computer Vision and Pattern Recognition*, pp. 14313–14323, 2024.

605 Yuzhang Shang, Bingxin Xu, Weitai Kang, Mu Cai, Yuheng Li, Zehao Wen, Zhen Dong, Kurt  
 606 Keutzer, Yong Jae Lee, and Yan Yan. Interpolating video-lmms: Toward longer-sequence lmms in a  
 607 training-free manner. *arXiv preprint arXiv:2409.12963*, 2024.

609 Jianlin Su, Murtadha Ahmed, Yu Lu, Shengfeng Pan, Wen Bo, and Yunfeng Liu. Roformer: Enhanced  
 610 transformer with rotary position embedding. *Neurocomputing*, 568:127063, 2024.

611 Xi Tang, Jihao Qiu, Lingxi Xie, Yunjie Tian, Jianbin Jiao, and Qixiang Ye. Adaptive keyframe  
 612 sampling for long video understanding. *arXiv preprint arXiv:2502.21271*, 2025.

614 Hugo Touvron, Thibaut Lavrille, Gautier Izacard, Xavier Martinet, Marie-Anne Lachaux, Timothée  
 615 Lacroix, Baptiste Rozière, Naman Goyal, Eric Hambro, Faisal Azhar, et al. Llama: Open and  
 616 efficient foundation language models. *arXiv preprint arXiv:2302.13971*, 2023a.

617 Hugo Touvron, Louis Martin, Kevin Stone, Peter Albert, Amjad Almahairi, Yasmine Babaei, Nikolay  
 618 Bashlykov, Soumya Batra, Prajjwal Bhargava, Shruti Bhosale, et al. Llama 2: Open foundation  
 619 and fine-tuned chat models. *arXiv preprint arXiv:2307.09288*, 2023b.

621 Peng Wang, Shuai Bai, Sinan Tan, Shijie Wang, Zhihao Fan, Jinze Bai, Keqin Chen, Xuejing Liu,  
 622 Jialin Wang, Wenbin Ge, et al. Qwen2-vl: Enhancing vision-language model’s perception of the  
 623 world at any resolution. *arXiv preprint arXiv:2409.12191*, 2024a.

624 Weihan Wang, Zehai He, Wenyi Hong, Yean Cheng, Xiaohan Zhang, Ji Qi, Xiaotao Gu, Shiyu Huang,  
 625 Bin Xu, Yuxiao Dong, et al. Lvbench: An extreme long video understanding benchmark. *arXiv*  
 626 *preprint arXiv:2406.08035*, 2024b.

627 Xiao Wang, Qingyi Si, Jianlong Wu, Shiyu Zhu, Li Cao, and Liqiang Nie. Adaretake: Adaptive  
 628 redundancy reduction to perceive longer for video-language understanding. *arXiv preprint*  
 629 *arXiv:2503.12559*, 2025.

631 Zhenzhi Wang, Limin Wang, Tao Wu, Tianhao Li, and Gangshan Wu. Negative sample matters: A  
 632 renaissance of metric learning for temporal grounding. In *Proceedings of the AAAI Conference on*  
 633 *Artificial Intelligence*, volume 36, pp. 2613–2623, 2022.

634 Hongchen Wei and Zhenzhong Chen. Visual context window extension: A new perspective for long  
 635 video understanding. *arXiv preprint arXiv:2409.20018*, 2024.

637 Hao Wu, Huabin Liu, Yu Qiao, and Xiao Sun. Dibs: Enhancing dense video captioning with unlabeled  
 638 videos via pseudo boundary enrichment and online refinement. In *Proceedings of the IEEE/CVF*  
 639 *conference on computer vision and pattern recognition*, pp. 18699–18708, 2024a.

640 Haoning Wu, Dongxu Li, Bei Chen, and Junnan Li. Longvideobench: A benchmark for long-context  
 641 interleaved video-language understanding. *Advances in Neural Information Processing Systems*,  
 642 37:28828–28857, 2024b.

643 Jin Xu, Zhifang Guo, Jinzheng He, Hangrui Hu, Ting He, Shuai Bai, Keqin Chen, Jialin Wang, Yang  
 644 Fan, Kai Dang, et al. Qwen2. 5-omni technical report. *arXiv preprint arXiv:2503.20215*, 2025.

646 Boqiang Zhang, Kehan Li, Zesen Cheng, Zhiqiang Hu, Yuqian Yuan, Guanzheng Chen, Sicong Leng,  
 647 Yuming Jiang, Hang Zhang, Xin Li, et al. Videollama 3: Frontier multimodal foundation models  
 for image and video understanding. *arXiv preprint arXiv:2501.13106*, 2025.

648 Hang Zhang, Xin Li, and Lidong Bing. Video-llama: An instruction-tuned audio-visual language  
 649 model for video understanding. *arXiv preprint arXiv:2306.02858*, 2023.  
 650

651 Peiyuan Zhang, Kaichen Zhang, Bo Li, Guangtao Zeng, Jingkang Yang, Yuanhan Zhang, Ziyue  
 652 Wang, Haoran Tan, Chunyuan Li, and Ziwei Liu. Long context transfer from language to vision.  
 653 *arXiv preprint arXiv:2406.16852*, 2024a.

654 Yuanhan Zhang, Jinming Wu, Wei Li, Bo Li, Zejun Ma, Ziwei Liu, and Chunyuan Li. Video  
 655 instruction tuning with synthetic data. *arXiv preprint arXiv:2410.02713*, 2024b.  
 656

## 658 A THE USE OF LARGE LANGUAGE MODELS(LLMs)

660 We used LLMs to assist in language polishing and grammar checking during the submission of the  
 661 manuscript.  
 662

## 664 B ISSUES OF MROPE AND PROOF

666 TIM primarily solves the MRoPE issue of Qwen2.5vl in a training-free way, meanwhile enabling the  
 667 understanding of absolute time.  
 668

- 669 1. For intervals shorter than 1 second, it directly rounds the value (e.g., frames corresponding  
 670 to 0.5s and 0.6s are encoded sequentially as  $a, a + 1$ ), which completely loses the concept  
 671 of absolute time.
- 672 2. Its absolute time encoding shows almost no capability for absolute time perception. Ad-  
 673 ditionally, for long videos, it wastes a large number of position IDs and causes relative  
 674 positional ambiguity.

### 676 B.1 RELATIVE POSITIONAL AMBIGUITY OF MROPE IN QWEN-2.5VL

678 In long video understanding, sparse sampling is commonly used to reduce computation, such as  
 679 sampling one frame per second. In this case, the position indices are often incremented uniformly  
 680 (e.g., at seconds 0, 20, 40, ...). Therefore, for Qwen2.5VL's MRoPE, **high-frequency dimensions** in  
 681 RoPE suffer from **rotational aliasing**, which leads to **relative positional ambiguity**.

682 RoPE encodes each position  $k$  by rotating its feature vector by an angle:  
 683

$$684 \phi_i(k) = k \cdot \theta_i, \quad \text{where } \theta_i = 10000^{-2i/d}$$

686 For any two positions  $k_1, k_2$ , the relative positional difference is represented by the angle difference:  
 687

$$688 \Delta\phi_i = (k_2 - k_1) \cdot \theta_i = \Delta k \cdot \theta_i$$

690 For a large position difference  $\Delta k$ , the frequency parameter  $\theta_i$  decreases rapidly with increasing  
 691 dimension  $i$ , which causes high-frequency dimensions to be more sensitive to position differences.

692 When the angle difference  $\Delta\phi_i$  exceeds  $2\pi$ , i.e., when the rotation completes a full cycle, RoPE maps  
 693 the positions  $k_1$  and  $k_2$  to the same phase, leading to a loss of relative positional information.

694 Let  $d = 256$  and the position interval be  $\Delta k = 20s$ . We compare two representative dimensions:  
 695

696 **Low-Frequency Dimension ( $i = 127$ ):**  
 697

$$698 \theta_{127} = 10000^{-\frac{2 \cdot 127}{256}} \approx 10^{-1.98} \approx 0.0105$$

$$699 \Delta\phi_{127} \approx 20 \cdot 0.0105 = 0.21 \text{ rad}$$

700 Since the period of low frequencies is long, it can still be distinguished quite well.  
 701

702 **High-Frequency Dimension ( $i = 0$ ):**

$$\theta_0 = 10000^{-\frac{2.0}{256}} = 1$$

$$\Delta\phi_0 = 20 \cdot 1 = 20 \text{ rad}$$

703 In this case, the angle difference  $\Delta\phi_0 = 20 \text{ rad}$  corresponds to approximately  $\frac{20}{2\pi} \approx 3.18$  full  
704 rotations. This may cause the relative position between two consecutive frames to become blurred.  
705

## 706 B.2 CRITICAL VALUE FOR MAINTAINING RELATIVE POSITIONAL RELATIONSHIP

707 In RoPE, the position encoding is given by rotating the feature vector by an angle  $\phi_i(k)$  for position  
708  $k$ . The frequency parameter  $\theta_i$  for dimension  $i$  is defined as:

$$\theta_i = 10000^{-2i/d}$$

709 where  $d$  is the total number of dimensions, and  $i$  is the index of the current dimension.  
710

711 For the highest-frequency dimension ( $i = 0$ ), the frequency is maximum:

$$\theta_0 = 10000^0 = 1$$

712 Thus, for  $i = 0$ , the rotation angle for a given position difference  $\Delta k$  is:

$$\Delta\phi_0 = \Delta k \cdot \theta_0 = \Delta k$$

713 The rotation angle  $\Delta\phi_0$  must remain within one period, i.e., within  $2\pi$  radians. Therefore, we require:  
714

$$\Delta\phi_0 < 2\pi$$

715 Substituting  $\Delta\phi_0 = \Delta k$ , we get:

$$\Delta k < 2\pi \approx 6.2832$$

716 For long videos, according to the Qwen2.5-vl method, the sampling interval can easily exceed this  
717 limit.  
718

## 719 C EXPERIMENTS ON OTHER MODELS

720 Table 4: Performance comparison on long video benchmark base on different models, including  
721 Video-MME (w/o subtitles), LongVideoBench, and LVBench. For fairly comparison, we re-test the  
722 model, with all video inputs preprocessed based on 4FPS and 448 resolution, and chose the supported  
723 64-frame limit for sampling (both LLAVA-onevision and InternVL3 are up to 64 frames). (♣: official  
724 reported results. ♦: we re-test results). For InternVL3, we use their official inference codes, but it  
725 has a significant gap compared with their reported results

726 Models	727 Size	728 Frames	729 Video-MME (w/o sub)		730 LongVideoB	731 LVBench
			732 Long (30-60min)	733 Overall (0-60m)	734 val (8s-3600s)	735 val (avg.>4000s)
736 LLAVA-onevision-7B♣	7B	64	-	58.2	56.3	-
737 LLAVA-onevision-7B♦	7B	64	47.88	57.90	40.54	57.14
738 w/ DATE	7B	64	48.11	58.62	45.12	58.56
739 InternVL3-8B ♣	8B	64	-	66.3	58.8	-
740 InternVL3-8B ♦	8B	64	50.55	61.81	54.90	43.45
741 w/ DATE	8B	64	53.00	62.44	59.31	46.03

## 742 D LIMITATIONS

743 Although DATE is an effective approach for enhancing absolute temporal understanding, it still  
744 encounters efficiency challenges when dealing with extremely long videos. The reliance on frame-  
745 level similarity computation and greedy selection under temporal constraints leads to an inference  
746 time that grows approximately linearly with video length. This may result in noticeable latency  
747 for hour-long videos—though such delays primarily occur during the initial pass, and subsequent  
748 interactions can leverage cached results for near-instant sampling. While reducing the sampling FPS  
749 can improve speed, it inevitably compromises precision. Future work may explore more scalable  
750 sampling strategies or hierarchical indexing mechanisms to improve runtime efficiency without  
751 sacrificing the model’s ability to locate temporally critical events.  
752

## E TASS DEMO

This is the detail sampling visualization of Fig.2, with 16 sampled red points and sampling orders labeled.

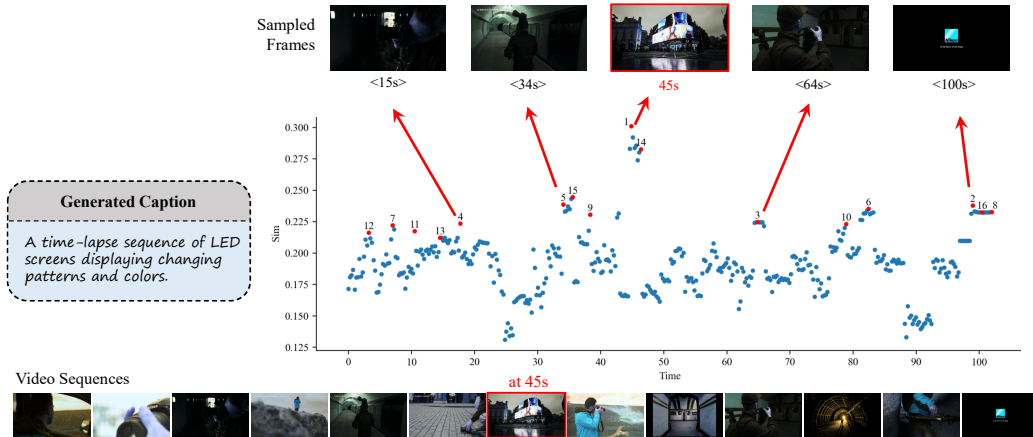


Figure 8: Sampling visualization.

810 F QUALITATIVE RESULTS AND ANALYSIS  
811

816 We present qualitative results to show the abilities of DATE-7B compared with Qwen2.5-VL-7B  
817 across various video understanding benchmarks. Fig.9,10,11,12,13,14 shows qualitative results on  
818 Video-MME, LVBench, and LongVideoBench.

819  
820  
821  
822  
823  
824  
825  
Source: Video-MME (cy40D1zOUow.mp4)

## 826 Question:

827 What is the third baked food in the video?

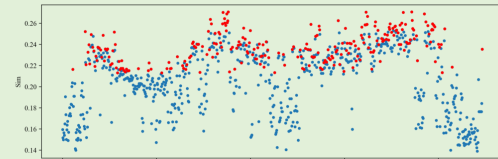
## 828 Options:

829 A. Scallop.  
830 B. Kobe beef.  
831 C. Bacon.  
832 D. Salmon.

833 Qwen2.5-VL: B  DATE (ours): C

## 834 Generated Caption:

835 A plated dish with a baked item, positioned third in a sequence of foods.



836 Sampled Frames

837 Source: Video-MME (cy40D1zOUow.mp4)



## 838 Question:

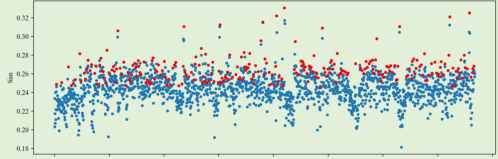
839 In which period does the home team overtake the guest team?

## 840 Options:

841 A. 12:56 - 8:13.  
842 B. 5:58 - 2:57.  
843 C. 8:13 - 5:58.  
844 D. 13:10 - 10:37.

845 Qwen2.5-VL: C  DATE (ours): B

## 846 Generated Caption:

847 The home team's score surpasses the guest team's score during a  
848 segment of the game.

849 Sampled Frames

850 Source: Video-MME (tXb\_zrHp4H8.mp4)



## 851 Question:

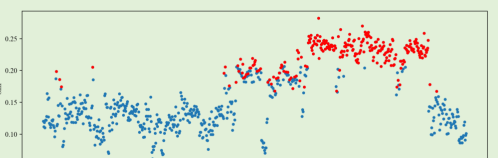
852 In which part of the video is the woman in the blue top interviewed?

## 853 Options:

854 A. Cannot be determined.  
855 B. The beginning of the video.  
856 C. The middle part of the video.  
857 D. The latter part of the video.

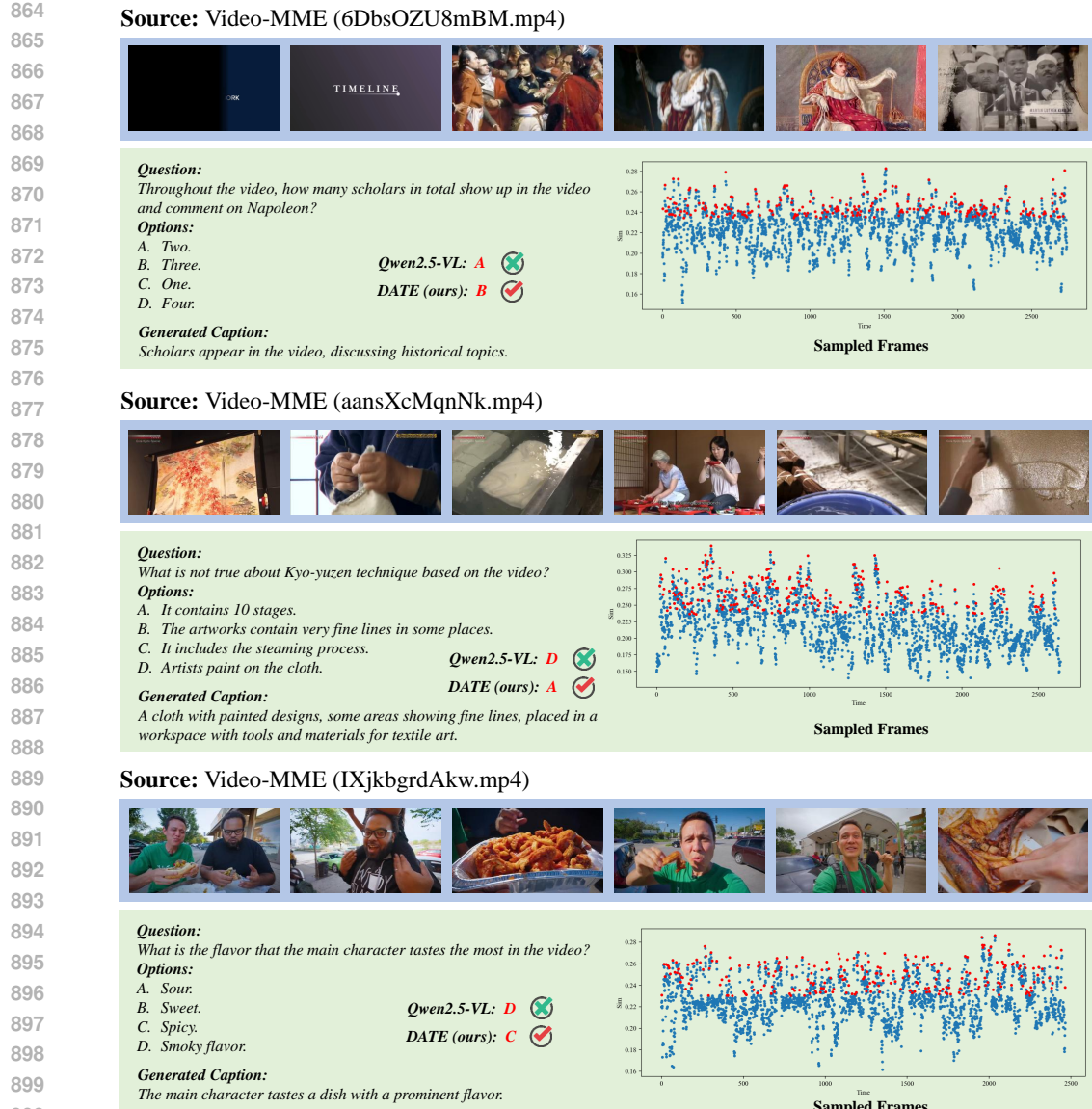
858 Qwen2.5-VL: B  DATE (ours): D

## 859 Generated Caption:

860 A woman in a blue top is seated, speaking to an interviewer in a  
861 studio setting.

862 Sampled Frames

863 Figure 9: Qualitative Results on Video-MME compared with Qwen2.5-VL-7B (1).





972  
973  
974  
975  
976**Source:** LVBench (T1yhBv1ytzw.mp4)977  
978  
979  
980  
981  
982**Question:**

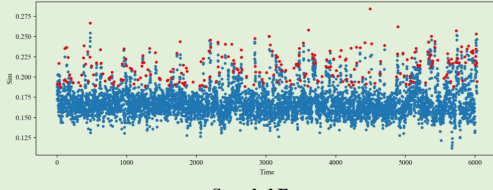
At 06:06, considering the player's facial expressions, whose belief and confidence is a little bit down?

**Options:**

A. Thiago  
B. Gomez  
C. Alisson  
D. Salah.

**Qwen2.5-VL:** *B*   
**DATE (ours):** *D* **Generated Caption:**

A player with a slightly downcast expression, appearing less confident.



Sampled Frames

983  
984  
985**Source:** LVBench (xECIRjlxM3U.mp4)986  
987  
988  
989  
990  
991  
992  
993  
994**Question:**

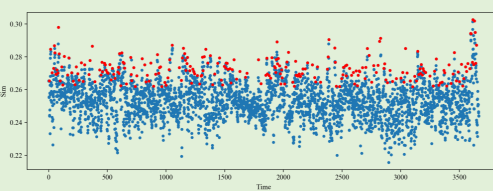
What year appears in the opening caption of the video?

**Options:**

A. 1636  
B. 1366  
C. 1363  
D. 1633.

**Qwen2.5-VL:** *A*   
**DATE (ours):** *D* **Generated Caption:**

A numerical year appears in the opening caption.



Sampled Frames

995  
996**Source:** LVBench (Cm73ma6Ibcs.mp4)997  
998  
999  
1000  
1001  
1002  
1003  
1004  
1005  
1006  
1007  
1008  
1009  
1010  
1011  
1012  
1013  
1014  
1015  
1016  
1017  
1018  
1019  
1020  
1021  
1022  
1023  
1024  
1025**Question:**

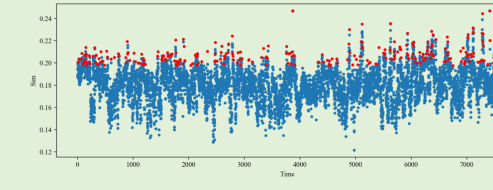
What words are written in the background for an event that involves a group of princesses or royal girls?

**Options:**

A. The contest  
B. The decision  
C. The conceal  
D. The competition.

**Qwen2.5-VL:** *D*   
**DATE (ours):** *A* **Generated Caption:**

A banner with decorative text in the background.



Sampled Frames

Figure 12: Qualitative Results on LVbench compared with Qwen2.5-VL-7B (2).

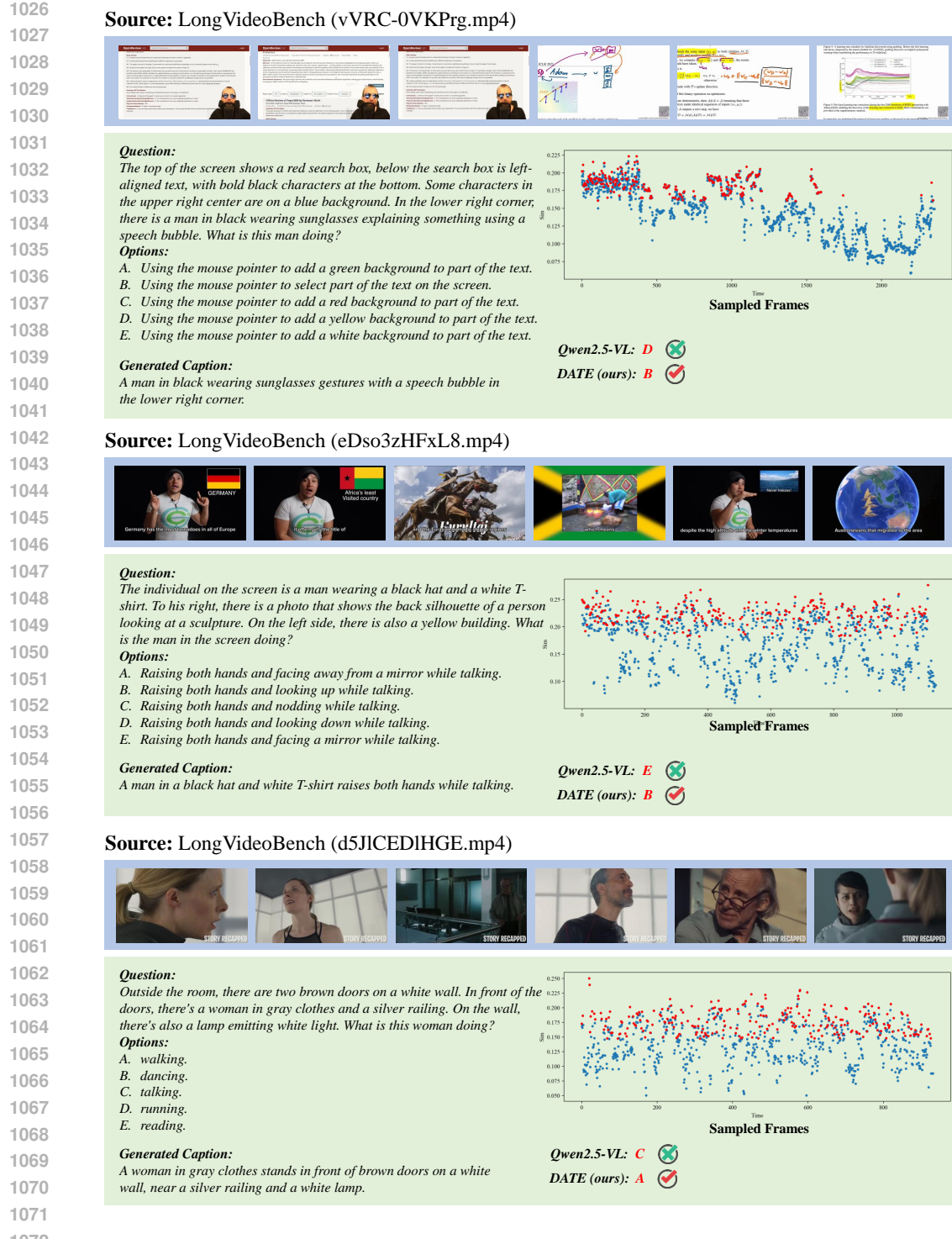


Figure 13: Qualitative Results on LongVideoBench compared with Qwen2.5-VL-7B (1).

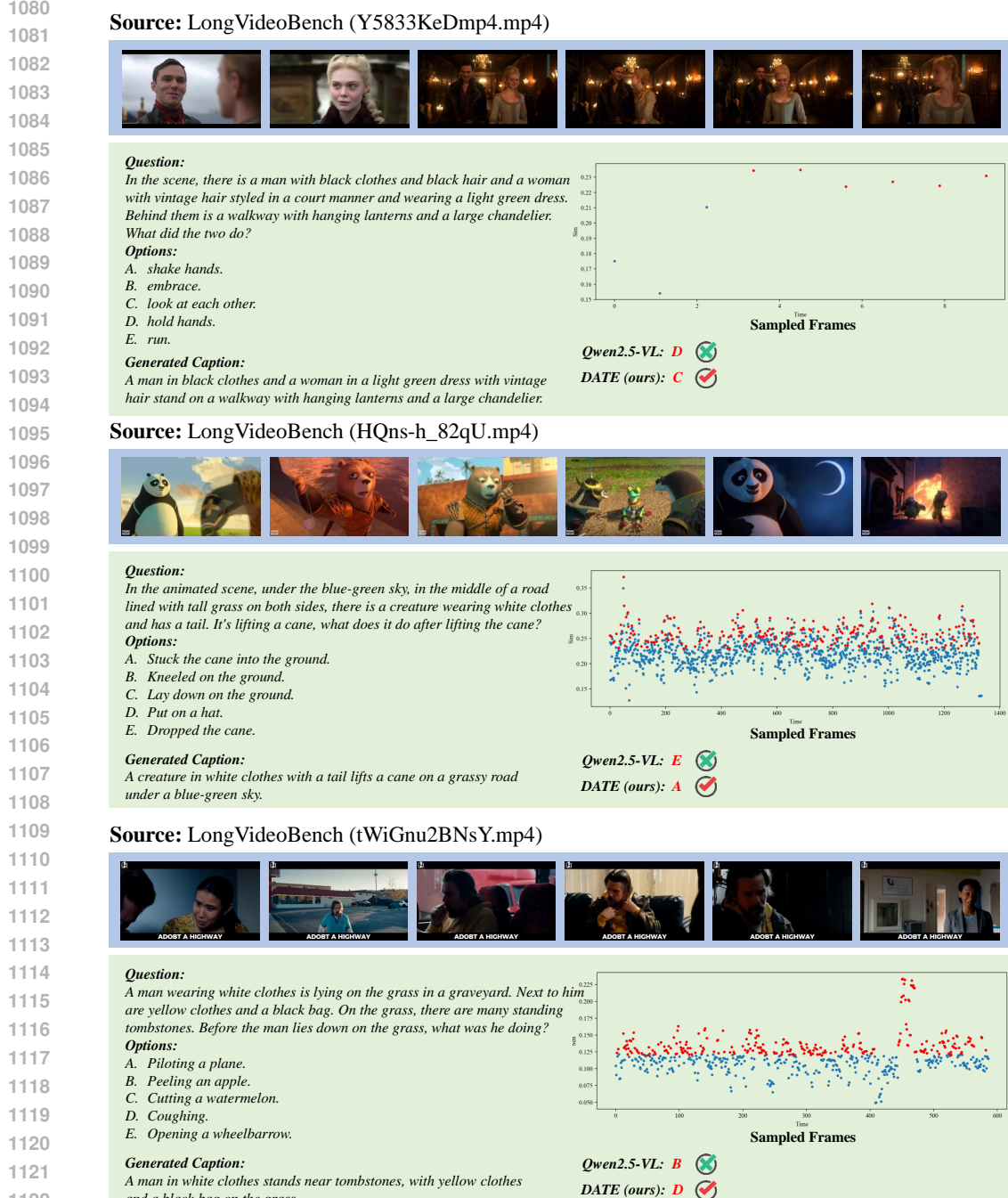
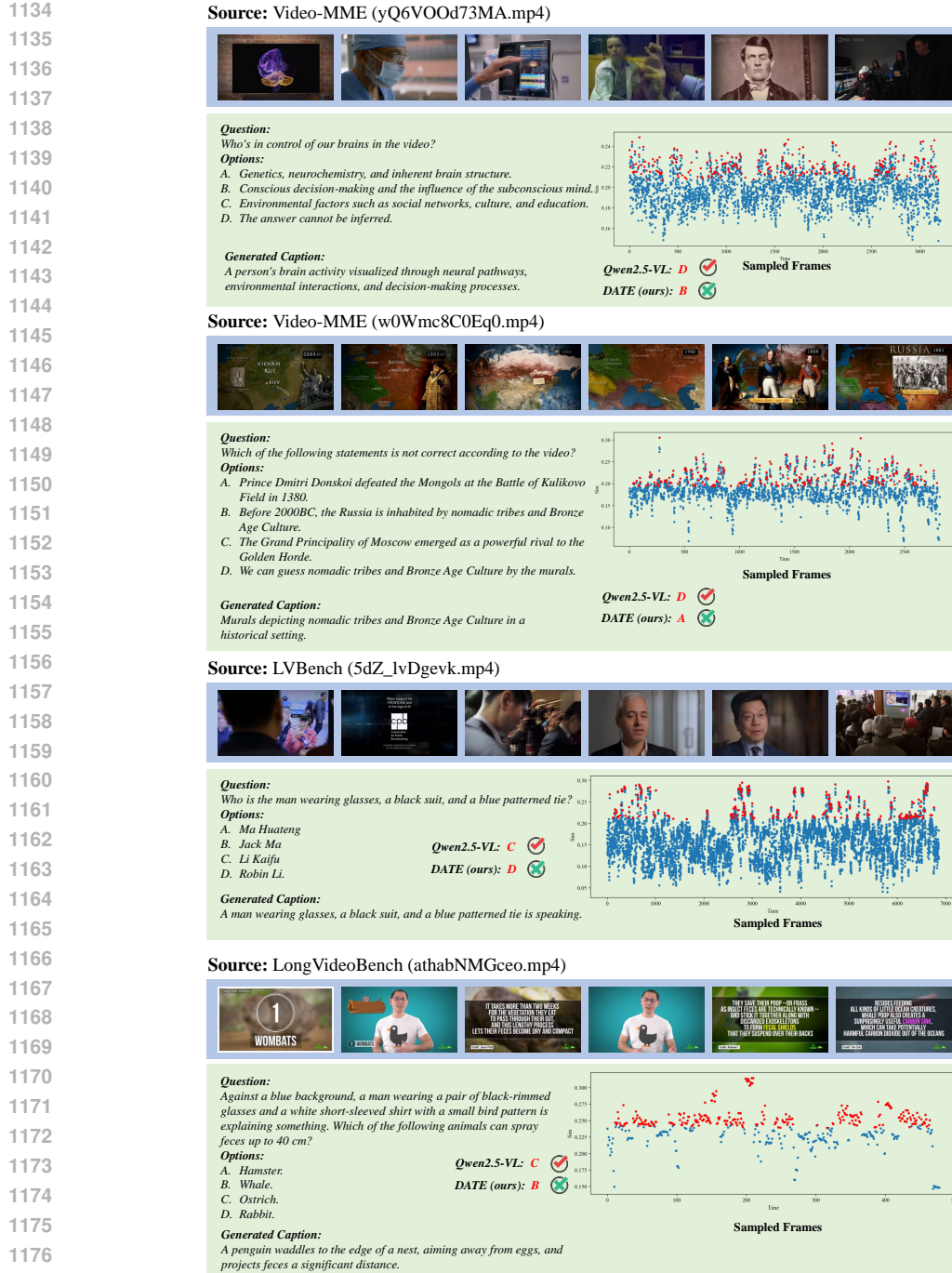


Figure 14: Qualitative Results on LongVideoBench compared with Qwen2.5-VL-7B (2).

## G BAD CASES

While we obtained good boosts across the three benchmarks, we instead made errors compared to the baseline predictions in some cases, as shown in Fig.15. We believe this may be due to the fact that we introduced additional tokens that increased the processing difficulty of the model, bringing it close to the upper limit of its capacity, thus increasing illusions for certain scenario.



1188 **H CAPTION GENERATION PROMPTS OF TASS**  
11891190 **Prompt**  
11911192 You are an image description assistant. Assume you are currently watching a video, and I will  
1193 give you a question related to the video.  
11941195 Your task is to generate potential image caption based on the question, which is able to find the  
1196 key image to answer the question.  
11971198 Core requirements:  
11991200 1. The output must be concise, objective, and visually observable facts.  
1201 2. Exclude subjective judgments, invisible information, and the specific content the question is  
1202 asking.  
1203 3. Avoid using quantities; use implicit references instead.  
1204 4. The question options given are for reference, you can use their commonalities, but not only one  
1205 of them.  
1206 5. Keep the output within 30 words.  
12071208 Output format:  
12091210 Directly output the visual description without any explanations or annotations.  
1211

1212 Here is the question: {question}

1213 Output Key Image Caption:

1214 **I DEMO WITH DIFFERENT TRAINING-FREE TIME EMBEDDINGS**  
12151216 **Q: At what time the women light the fire?**  
1217

Setting	Inputs	Answer
Base	<v><v>...<v><v>Q	The woman lights the fire at approximately 23 seconds into the video.
Prompt	<v><v>...<v><v>Here are the timestamps of the given video:<0.0s><0.8s>...<27.0s>`n Q	The woman lights the fire at 22.6 seconds.
Label frame and prompt	<1><v><2><v>...<31><v><32><v>Here are the timestamps of each frame:<0.0s><0.8s>...<27.0s>`n Q	The woman lights the fire at 27.0 seconds into the video.
TIM (start)	<0.0s><v><0.8s><v>...<26.1s><v><27.0s><v>Q	The woman lights the fire at 24.4 seconds into the video.
TIM (end)	<v><0.0s><v><0.8s><v>...<26.1s><v><27.0s>Q	The woman lights the fire at 25.2 seconds into the video.

1218 **Figure 16: Compare TIM with MROPE (base), timestamps given in prompts, mark frames and given  
1219 timestamps in prompt, TIM with time at the start of the vision tokens, and TIM with time at the end  
1220 of the vision tokens. It shows that both at the start/end of the vision segment is available for  
1221 MLLM to understand a relatively absolute time.**  
12221223  
1224  
1225  
1226  
1227  
1228  
1229  
1230  
1231  
1232  
1233  
1234  
1235  
1236  
1237  
1238  
1239  
1240  
1241